



Cite this: *Polym. Chem.*, 2025, **16**, 3675

Received 10th June 2025,
Accepted 31st July 2025

DOI: 10.1039/d5py00583c

rsc.li/polymers

The stereocontrolled synthesis of poly(1-butene) has been established using metallocene catalysts in the field of homogeneous catalysis. However, there are few reports on the efficient and controllable polymerization of 1-butene using non-metallocene catalysts, possibly due to the limited strategies for generating stereospecific active species specifically for high-carbon α -olefins. In this study, a series of novel tridentate $[\text{O}^-\text{NX}]$ titanium complexes were designed and used to synthesize poly(1-butene) materials with high activity (up to $3.41 \times 10^6 \text{ g mol}^{-1} \text{ h}^{-1}$), ranging from atactic to isotactic (up to 91% *mmmm*). The physical properties of the obtained poly(1-butene) materials were highly correlated with their isotacticity, and highly isotactic poly(1-butene) possessed good toughness.

Introduction

Isotactic poly(1-butene) is a semi-crystalline polyolefin with exceptional properties, including a high heat distortion temperature, high creep resistance, good impact resistance and superior toughness, and it has been successfully industrialized and applied in food packing and hot-water pipes.^{1–3} Meanwhile, atactic and moderately isotactic poly(1-butene) have shown potential applications as adhesives and elastomers.^{4,5} Poly(1-butene) was initially produced by Natta in 1955,^{6,7} and its controllable synthesis has received more attention since the 1980s thanks to the remarkable development of single-site metallocene catalysts.^{8–27} In 1985, Kaminsky used *ansa*-zirconocene **1** to furnish poly(1-butene) with activity of $2.64 \times 10^6 \text{ g mol}^{-1} \text{ h}^{-1}$ with a high isotacticity index determined by IR spectroscopy (Chart 1, **1**).²⁸ In 2006, Resconi

developed a series of *ansa*-zirconocenes **2**,²⁹ which produced poly(1-butene) with activity of over $10^8 \text{ g mol}^{-1} \text{ h}^{-1}$ with isotacticities of 78–96% *mmmm* (Chart 1, **2**). Though catalyst performance is no longer a question regarding the industrialization of metallocene-catalyzed poly(1-butene),³⁰ commercially available products are still rare. Non-metallocene^{31–38} catalysts can be prepared with diverse ligand skeletons, however, their application in 1-butene polymerization has not concurrently shown good polymerization activity and isotacticity. In 2003, Miyatake utilized thiobis(phenoxy)titanium **3** and water/ $\text{C}_6\text{F}_5\text{OH}$ -modified MMAO to yield poly(1-butene) with good activity ($1.26 \times 10^6 \text{ g mol}^{-1} \text{ h}^{-1}$) and mediocre isoselectivity (30% *mmmm*) (Chart 1, **3**).³⁹ In 2005, Pellecchia achieved 1-butene polymerization by employing salen zirconium **4**, which exhibited low activity ($7.40 \times 10^2 \text{ g mol}^{-1} \text{ h}^{-1}$) and moderate isoselectivity (60% *mmmm*) (Chart 1, **4**).⁴⁰ Subsequently, Pellecchia developed the tridentate $[\text{O}^-\text{NN}]$ zirconium complex **5** for the polymerization of 1-butene, and this increased the isotacticity of the resulting polymer to 87% *mmmm*, albeit with low activity ($9.70 \times 10^2 \text{ g mol}^{-1} \text{ h}^{-1}$) (Chart 1, **5**).⁴¹ Mechanistic studies prove that the ligand of the active species becomes diaionic from dehydrochlorination, constructing a covalent bond between $\text{sp}^3\text{-N}$ and the Zr center. Thus, there are still sig-

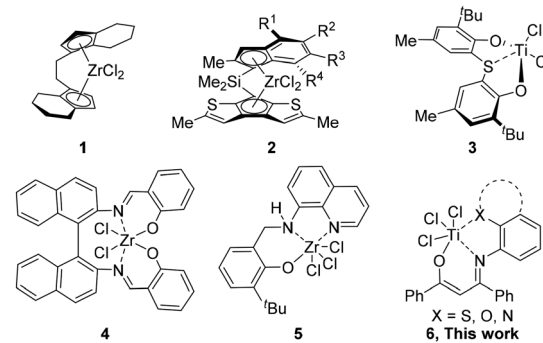


Chart 1 Representative single-site catalysts investigated for the synthesis of isotactic poly(1-butene).

^aKey Laboratory of Photoelectric Conversion and Utilization of Solar Energy, Qingdao Institute of Bioenergy and Bioprocess Technology, Chinese Academy of Sciences, Qingdao, 266101, China. E-mail: taowj@qibebt.ac.cn, wangqq@qibebt.ac.cn

^bShandong Energy Institute, Qingdao, 266101, China

^cCenter of Materials Science and Optoelectronics Engineering, University of Chinese Academy of Sciences, Beijing, 100049, China

†These authors contributed equally to this work.



nificant challenges in developing non-metallocene catalysts to achieve the efficient, low-cost, and controllable production of poly(1-butene).

To this end, a mechanistic understanding of stereoregularity control when using single-site catalysts^{8–27,31–38,42} is important. In an *ansa*-metallocene catalyst system, the *C*₂-symmetric active species achieves isotactic polymerization through the alternation of polymer chain growth between the two identical face-selective sites.⁴³ Meanwhile, the isotactic preference of *C*₁-symmetric species originates from the site epimerization of the polymer chain and the face selectivity of the unique coordination site.^{44,45} Although these stereochemical principles are also applicable to group-IV non-metallocene catalysts,^{31–38,46,47} most of them exhibit low activity towards high-carbon α -olefin polymerization due to their congested tetracoordinate environment in *C*₂- or *C*₁-symmetric systems. In contrast, tridentate group-IV complexes, such as (pyridylamido)Hf discovered by Dow and Symyx in 2003, exhibit excellent activity and isoselectivity during α -olefin polymerization.^{48–57} Coates proposed that the isoselectivity of these *C*_s-symmetric tridentate hafnium complexes was caused by unexpected *in situ* monomer insertion into the Hf–C_{aryl} bond, leading to *C*₁-symmetric active species.⁵⁸ Similarly, a *C*₁-symmetric $[(N^-\text{NN}^-)\text{Zr}(\mu\text{-H})_n\text{Al}^{\text{I}}\text{Bu}_2]^+$ species was proposed to affect stereoselectivity in Pellecchia's tridentate *C*_s-symmetric $[\text{N}^-\text{NN}^-]$ zirconium complexes,^{59,60} which was also supported by a computational study by Talarico.⁶¹ A rare tridentate hafnium catalyst reported by Voskoboinikov in 2021 showcased high isoselectivity with its *C*₂ symmetry formed by the rigid ligand skeleton.⁶² Notably, most tridentate non-metallocene catalysts involved in the stereoselective polymerization of α -olefins employed dianionic ligands. To the best of our knowledge, the field of α -olefin polymerization remains unexplored in terms of tridentate non-metallocene catalysts with a monoanionic ligand,^{63–80} particularly regarding their potential for stereoregularity control.

Herein, we report that a tridentate titanium complex family with a $[\text{O}^-\text{NX}]$ ligand can catalyze stereoselective 1-butene polymerization to produce poly(1-butene), from atactic to isotactic (up to 91% *mmmm*), with high activity (up to $3.41 \times 10^6 \text{ g mol}^{-1} \text{ h}^{-1}$) and with different side-arm donors (Chart 1, 6). Compared with previous reports,^{48–62,83,84} this is the first report on the application of group-IV non-metallocene catalysts with a monoanionic ligand for the stereoselective polymerization of α -olefins.

Results and discussion

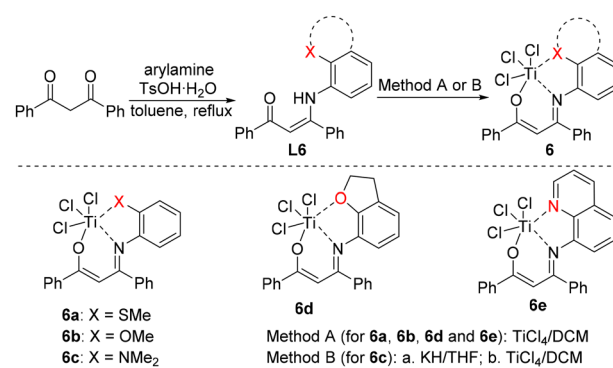
Tridentate $[\text{O}^-\text{NX}]$ titanium complexes, originally developed by Tang's group, have shown remarkable applications in the regulation of polyethylene structures and properties by employing different side-arm donors.^{70–82} We assume that tridentate $[\text{O}^-\text{NX}]$ titanium complexes with more open catalytic space are good candidates to catalyse the polymerization of 1-butene with high activity. In this research, a series of novel tridentate

$[\text{O}^-\text{NX}]$ titanium complexes is designed and thoroughly investigated for 1-butene polymerization.

Based on reported methods,⁷⁵ **L6** ligands were synthesized *via* the condensation of 1,3-diphenylpropane-1,3-dione and different substituted anilines. **L6** ligands were treated with titanium chloride to afford complexes **6a–6e** with side arms bearing S, O and N (Scheme 1), which were characterized carefully by ¹H NMR, ¹³C NMR and elemental analysis. Single crystals of complexes **6a**, **6c**, **6d** and **6e** were grown by the slow vapor diffusion of *n*-hexane into their toluene solutions. Single-crystal X-ray diffraction studies confirmed their structures.

As shown in Fig. 1,⁸⁵ complexes **6a**, **6c**, **6d** and **6e** feature distorted octahedral coordination at the titanium center, with three chlorine ligands in a *mer* arrangement. The N, O, Ti, X (side-arm heteroatom) and equatorial Cl are essentially in the same plane. Slight distortion was discovered between an X-containing five-membered ring (N1–C10–C15–S1–Ti1 in **6a**) and an O-containing six-membered ring (O1–C1–C2–C3–N1–Ti1 in **6a**). Interestingly, the single crystal of **6a** is a mixture of enantiomers at the chiral S atom, indicating that **6a** is actually *C*₁-symmetric (see SI, crystal data). The bond angle sum of C15–S1–C16 (102.9°), C15–S1–Ti1 (95.0°) and C16–S1–Ti1 (108.6°) is 306.5°, suggesting that the S atom in **6a** is *sp*³-hybridized. The bond angle sum of C22–O2–C21 (104.9°), Ti1–O2–C22 (130.7°) and Ti1–O2–C21 (110.7°) in **6d** is nearly 360°, revealing the near-*sp*²-hybridization of the O2 atom. The different hybridizations of S and O in the side arms are consistent with previous reports.⁷³ Both **6d** and **6e** are nearly planar, with similar Ti–X bond lengths (2.17 Å vs. 2.16 Å), which may lead to similar catalytic polymerization performance.

Complex **6a** with a pendant –SMe group was chosen as the model catalyst to optimize the 1-butene polymerization conditions, inspired by the excellent performance of S-containing tridentate $[\text{O}^-\text{NX}]$ titanium complexes for ethylene polymerization.^{70–82} Some representative results are summarized in Table 1. When using 500 equivalents of MMAO as the co-catalyst, the activity of 1-butene polymerization was $4.8 \times 10^4 \text{ g mol}^{-1} \text{ h}^{-1}$ (Table 1, entry 1), which is much lower than



Scheme 1 Synthetic pathways to the tridentate $[\text{O}^-\text{NX}]$ titanium complexes **6a–6e**.



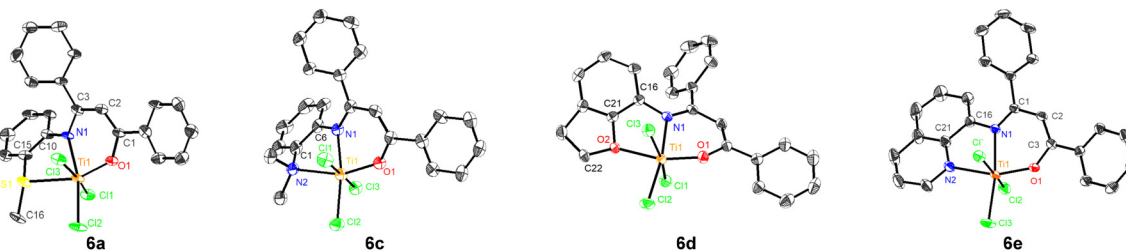


Fig. 1 Molecular structures of **6a**, **6c**, **6d** and **6e**. Selected bond lengths (Å) and angles (°): **6a**: Ti1–O1 1.833(6), Ti1–N1 2.137(7), Ti1–S1 2.595(2); S1–Ti1–N1 75.29(19), S1–Ti1–O1 159.2(2), N1–Ti1–O1 84.9(3); **6c**: Ti1–O1 1.852(5), Ti1–N1 2.102(6), Ti1–N2 2.306(6); N2–Ti1–N1 74.3(2), N2–Ti1–O1 157.5(2), N1–Ti1–O1 83.2(2); **6d**: Ti1–O1 1.8252(15), Ti1–N1 2.1551(16), Ti1–O2 2.1684(14); O2–Ti1–N1 74.40(6), O2–Ti1–O1 160.87(6), N1–Ti1–O1 84.49(6); **6e**: Ti1–O1 1.8262(14), Ti1–N1 2.1713(15), Ti1–N2 2.1616(18); N2–Ti1–N1 75.34(6), N2–Ti1–O1 159.72(6), N1–Ti1–O1 84.50(6). Hydrogen atoms are omitted for clarity. Thermal ellipsoids are set at 30% probability.

Table 1 Optimization of the reaction conditions for **6a**-catalyzed 1-butene polymerization^a

Entry	Co-cat.	[Al]/[Ti]/ [B]	Time (min)	Yield (g)	Act. ^b (10^5 g mol $^{-1}$ h $^{-1}$)	M_n ^c (kDa)	D ^c
1	MMAO	500/1/0	120	0.96	0.48	11	2.4
2	MMAO	1000/1/0	120	1.63	0.82	24	2.1
3	MMAO	2000/1/0	120	0.98	0.49	27	2.2
4	MAO	1000/1/0	120	1.13	0.57	9	3.2
5	AlMe ₃ /[Ph ₃ C][B(C ₆ F ₅) ₄]	50/1/1	120	1.50	0.75	49	2.1
6	Al ⁱ Bu ₃ /[Ph ₃ C][B(C ₆ F ₅) ₄]	50/1/1	120	1.13	0.57	37	2.5
7	AlEt ₃ /[Ph ₃ C][B(C ₆ F ₅) ₄]	50/1/1	120	2.50	1.25	7	2.5
8	AlEt ₃ /[Ph ₃ C][B(C ₆ F ₅) ₄]	50/1/1	30	2.43	4.86	8	2.4
9 ^d	AlEt ₃ /[Ph ₃ C][B(C ₆ F ₅) ₄]	50/1/1	30	3.68	7.36	14	2.2
10 ^d	AlEt ₃ /[Ph ₃ C][B(C ₆ F ₅) ₄]	25/1/1	30	3.76	7.52	38	2.3
11 ^d	AlEt ₃ /[Ph ₃ C][B(C ₆ F ₅) ₄]	10/1/1	30	2.32	4.64	163	2.5

^a Reaction conditions: 1-butene (2.4–2.5 g), **6a** (0.01 mmol in 2 mL of toluene), co-catalyst, 25 °C, 30–120 min, in a sealed tube, quenched by acidified ethanol at the set time. ^b Activity is in units of 10^5 g mol $^{-1}$ h $^{-1}$.

^c Determined via GPC. ^d 4.8–4.9 g of 1-butene was used.

that of reported ethylene polymerization. Increasing the Al/Ti ratio from 500 to 1000 improved the activity obviously (Table 1, entry 2). However, further increasing the Al/Ti ratio to 2000 had a negative effect on activity (Table 1, entry 3). MAO as the cocatalyst resulted in low activity (5.7×10^4 g mol $^{-1}$ h $^{-1}$) when the Al/Ti ratio was 1000 (Table 1, entry 4). To our delight, it was found that employing alkyl aluminum and [Ph₃C][B(C₆F₅)₄] as co-catalysts resulted in higher activity (Table 1, entries 5–7), and the Al/Ti ratio can be reduced to 50. AlEt₃ facilitated complete monomer conversion within 120 min with an activity of 1.25×10^5 g mol $^{-1}$ h $^{-1}$ (Table 1, entry 7). By shortening the reaction time (Table 1, entry 8) and increasing the monomer loading (Table 1, entry 9), the activity can reach 7.36×10^5 g mol $^{-1}$ h $^{-1}$. Reducing the Al/Ti ratio from 50 to 25 (Table 1, entry 10) resulted in a higher activity (7.52×10^5 g mol $^{-1}$ h $^{-1}$) and molecular weight (38 kDa). However, further reducing the Al/Ti ratio to 10 (Table 1, entry 11) resulted in a loss of activity (4.64×10^5 g mol $^{-1}$ h $^{-1}$) with a higher molecular weight (163 kDa). Of note, an induction period was needed, since sticky reaction mixtures and an exothermic phenomenon will not be observed until 15 min after the addition of [Ph₃C][B(C₆F₅)₄]. In summary, we used model complex **6a** and success-

fully optimized the 1-butene polymerization conditions. Interestingly, we can employ alkyl aluminum (25 eq.) and [Ph₃C][B(C₆F₅)₄] (1.0 eq.) as cocatalysts to replace costly MAO or MMAO and produce poly(1-butene) efficiently.

With the best polymerization conditions in hand (Table 1, entry 10), 1-butene polymerizations using catalysts **6** with different side-arm donors were further investigated, as shown in Table 2. Atactic poly(1-butene) was obtained by using **6a** (Table 2, entry 1) in the form of a viscous oil. Complex **6b** bearing an -OMe group gave a slightly lower activity (3.92×10^5 g mol $^{-1}$ h $^{-1}$) and moderate isotacticity (44% *mmmm*) (Table 2, entry 2), producing poly(1-butene) with elasticity. **6c**, with an sp³-N donor pendant group, did not yield observable polymers (Table 2, entries 3 and 4), whether using AlEt₃/[Ph₃C][B(C₆F₅)₄] or MMAO as cocatalysts, which agreed with previous reports regarding ethylene polymerization.⁶⁹ We speculate that an increase in poly(1-butene) isotacticity is possibly attributed to smaller steric hindrance from the -OMe group. As a result, we designed complex **6d** with an alkyl-constrained dihydrofuran structure. Interestingly, **6d** exhibited better isoselectivity (60% *mmmm*) and higher activity (6.00×10^5 g mol $^{-1}$ h $^{-1}$) compared with **6b** (Table 2, entry 5 vs. entry 2). Notably, lowering the reaction temperature to -20 °C further increased the isotacticity (80% *mmmm*) and polymerization activity, with the corresponding product taking the form of hard plastic (Table 2, entry 6). Given that a significant quantity of emitted heat was observed during the polymerization process, we speculate that at a lower temperature, such as -20 °C, the thermal decomposition of active species was avoided so that the polymerization activity was improved (Table 2, entry 6 vs. entry 5). When MMAO was used as a co-catalyst, the isotacticity was improved to 75% *mmmm*, although the activity (1.50×10^5 g mol $^{-1}$ h $^{-1}$) was reduced quite a lot (Table 2, entry 7 vs. entry 5). The performance of **6d** confirmed our hypothesis that smaller side-arms lead to better isoselectivity and activity. Next, we turned to modifying sp³-N in **6c** to sp²-N. Surprisingly, when -NMe₂ was replaced with pyridine to yield the complex **6e**, there was a remarkable increase in polymerization activity (2.60×10^6 g mol $^{-1}$ h $^{-1}$) and isotacticity (82% *mmmm*) (Table 2, entry 8 vs. entry 5). Boiling of the reaction mixture within a few seconds of the addition of [Ph₃C][B(C₆F₅)₄] was observed.



Table 2 Effects of the side arms on 1-butene polymerization^a

Entry	Side-arm (cat.)	Time (min)	Yield (g)	Act. ^b	M_n ^c (kDa)	D^c	$mmmm^d$
1	SMe (6a)	30	3.76	7.52	38	2.3	<10
2	OMe (6b)	30	1.96	3.92	57	2.0	44
3	NMe ₂ (6c)	120	n.r.	n.p.	—	—	—
4 ^e	NMe ₂ (6c)	120	n.r.	n.p.	—	—	—
5	Dihydrofuran (6d)	30	3.00	6.00	41	2.4	60
6 ^f	Dihydrofuran (6d)	30	3.28	6.56	129	2.1	80
7 ^e	Dihydrofuran (6d)	30	0.75	1.50	38	1.9	75
8	Pyridine (6e)	5	2.17	26.0	41	2.8	82
9 ^f	Pyridine (6e)	5	2.84	34.1	52	3.2	85
10 ^e	Pyridine (6e)	30	0.91	1.82	42	2.1	91

^a Reaction conditions: 1-butene (4.8–4.9 g), 6 (0.01 mmol in 2 mL of toluene), AlEt₃ (0.25 mmol, 1 M in hexane), [Ph₃C][B(C₆F₅)₄] (0.01 mmol in 2 mL of toluene), 25 °C, 5–30 min, in a sealed tube, quenched by acidified ethanol at the set time. ^b Activity is in units of 10⁵ g mol⁻¹ h⁻¹.

^c Determined via GPC. ^d Determined via quantitative ¹³C NMR spectrum analysis. ^e 10 mmol of MMAO was used instead of AlEt₃/[Ph₃C][B(C₆F₅)₄].

^f The reaction is run at –20 °C.

Consequently, the magnetic stirrer stopped stirring after 5 min due to the increased viscosity of the reaction solution. The poor stirring and high reaction viscosity of the mixtures may have led to the relatively wide PDI values (Table 2, entry 8: PDI = 2.8; entry 9: PDI = 3.2). Encouraged by the above findings, we tried 1-butene polymerization using catalyst **6e** at –20 °C and produced poly(1-butene) with increased activity (3.41 × 10⁶ g mol⁻¹ h⁻¹) and isotacticity (85% *mmmm*) (Table 2, entry 9). Of note, isotacticity can be further improved to 91% *mmmm* by using MMAO as the co-catalyst at room temperature, with reduced activity (1.82 × 10⁵ g mol⁻¹ h⁻¹) (Table 2, entry 10). To the best of our knowledge, the above experiment results represent the highest level of activity and isoselectivity obtained in non-metallocene-catalyzed 1-butene polymerization. **6e** avoids the use of expensive MAO and has a simple synthesis process; however, it still shows unsatisfactory activity and isoselectivity in 1-butene polymerization compared with metallocene catalysts.²⁹ More structural modifications of **6e** to enhance its practicality are currently underway in our lab.

The quantitative ¹³C NMR spectra of corresponding poly(1-butene) samples from Table 2 are shown in Fig. 2, ranging from isotactic to atactic. The *rrrr* pentad cannot be observed, implying that the resulting polymers are not hemi-isotactic. This suggests that consecutive migratory insertions between the axial site and the equatorial site are not feasible. On the other hand, *mmmr*, *mmrr*, and *mrrm* pentad peaks retain clear signals with increased tacticity, suggesting the prompt correction of stereoirregularity *via* an ESC mechanism¹⁹ and that site epimerization is likely operative. In addition, regioerror and chain-end peaks were not observed in any of the polymers.

To correlate poly(1-butene) isotacticities with physical properties, the thermal and mechanical properties of representative polymers were investigated. To minimize polymer molecular-weight effects on the physical properties, the samples fall within a comparable molecular weight range of 38–57 kDa (Table 2, entries 1, 2, 5, 8 and 10). Interestingly, good correlation was discovered between the glass-transition temperature (T_g) and the isotacticity, *i.e.*, the higher the isotacticity, the lower the T_g value (varying from –15.5 to –32.1 °C, Fig. 3a, a–

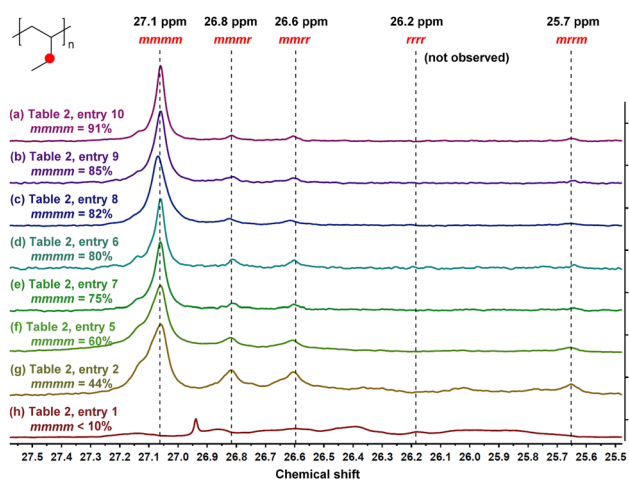


Fig. 2 Quantitative ¹³C NMR (298 K, CDCl₃) spectra analysis of the methylene carbon in the side chains of the obtained poly(1-butene) samples.

e), which suggested that the highly isotactic poly(1-butene) may have applications in a wide temperature range. This trend may be because the atactic amorphous structure reduced the mobility of the chain end, slowing down the transition kinetics. No T_m was found for low-isotacticity poly(1-butene) (Fig. 3b, a and b), indicating the low crystallinity of these polymers. More than one T_m peak was observed in moderately to highly isotactic poly(1-butene). The highest T_m values were positively correlated with the isotacticity of the corresponding polymers (varying from 71.8 to 81.8 °C, Fig. 3b, c–e). Moreover, an exothermic peak was discovered for 91% *mmmm* poly(1-butene) (Fig. 3b, e) at 23.9 °C with heating, indicating the occurrence of cold crystallization. We believe that highly isotactic poly(1-butene) does not crystallize during a direct cooling process; however, cold crystallization occurs during subsequent heating.

Fig. 3c shows 1D WAXD profiles of the above five examples aged at room temperature for 30 days. For low-isotacticity poly(1-butene) (Fig. 3c, a and b), crystalline peaks cannot be



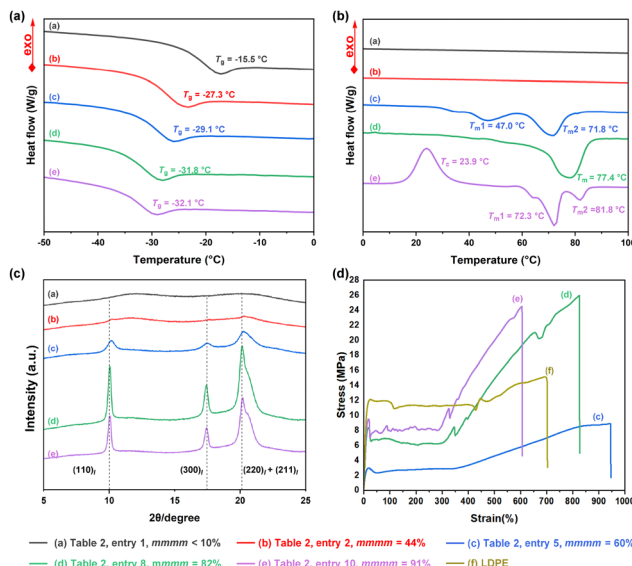


Fig. 3 Characterization of obtained poly(1-butene) samples. (a) DSC thermograms from the first heating cycle showing T_g . (b) DSC thermograms from the second heating cycle showing T_c and T_m . (c) Wide-angle X-ray diffraction (WAXD) profiles. (d) Stress-strain curves measured at a speed of 50 mm min^{-1} for all specimens after aging for 24 h.

observed clearly. The low-crystalline nature of these polymers was also supported by DSC analysis (Fig. 3b, a and b). As expected, when the isotacticity of poly(1-butene) is increased (Fig. 3c, c–e), the crystallization peaks of the corresponding poly(1-butene) samples become clear and sharp in the WAXD spectra, which indicated that the thermal properties were greatly affected by the isotacticity of the materials. In addition, the distinct diffraction peaks observed at 2θ values of 10.1° , 17.5° , and 20.2° corresponded to the (110), (300), and (220) + (211) crystallographic planes of hexagonal⁸⁶ form I, while peaks of other crystal forms are invisible, suggesting that a complete phase transition from tetragonal form II to hexagonal form I has been achieved.

Subsequently, we attempted to investigate the mechanical characteristics of poly(1-butene) with different isotacticities through tensile tests. It is noteworthy that only poly(1-butene) materials with medium to high isotacticity (Fig. 3d, c–e) could be successfully fashioned into tensile-test specimens, while sample a and b failed due to their excessive viscosity. 91% *mmmm* poly(1-butene) (Fig. 3d, e) showed the highest yield strength ($\sigma_Y = 9.5 \text{ MPa}$) but the lowest elongation at break ($\epsilon_B = 513\%$). Sample d with 82% *mmmm* isotacticity (Fig. 3d, d) was softer, with a yield strength of $\sigma_Y = 8.3 \text{ MPa}$ and an elongation at break of $\epsilon_B = 837\%$. Sample c with 60% *mmmm* (Fig. 3d, c) showed a marked decrease in yield strength ($\sigma_Y = 2.9 \text{ MPa}$) accompanied by the highest elongation at break value ($\epsilon_B = 946\%$). Compared to commercial LDPE (Fig. 3d, f; $\sigma_Y = 12.1 \text{ MPa}$, $\epsilon_B = 703\%$), poly(1-butene) with 82% *mmmm* isotacticity possesses much higher tensile strength (26.0 MPa *vs.* 15.1 MPa) and a larger area under the stress-strain curve, indicat-

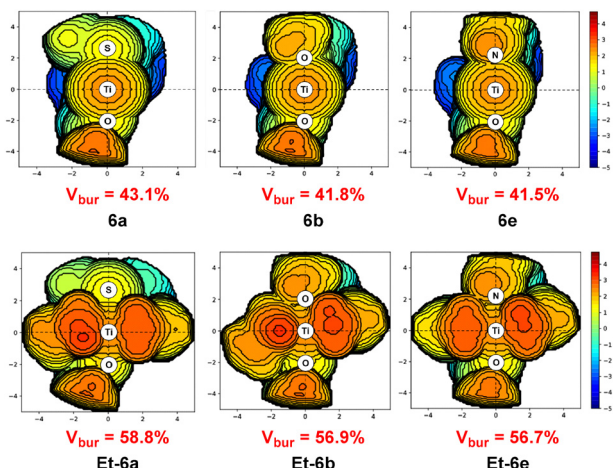


Fig. 4 A comparison of steric hindrance. Steric maps of **6a**, **6b** and **6e**, and their corresponding active species **Et-6a**, **Et-6b** and **Et-6e**. The titanium center is placed at the center of the xyz coordinate system. The Ti–N bond coincides with the z-axis. The y-axis represents the axial position of the xz-plane containing the titanium center. The chloride atoms are omitted in **6a**, **6b** and **6e**, and the ethyl groups are retained in **Et-6a**, **Et-6b** and **Et-6e**.

ing its good toughness and potential applications as a plastic film and packaging material.

To rationalize the remarkable effects of side-arm donors on stereocontrol, we first studied the steric hindrance effects and generated steric maps of complexes **6a**, **6b** and **6e** and their possible active species **Et-6a**, **Et-6b** and **Et-6e** using the SambVca 2.0 program⁸⁷ (Fig. 4). The structures of complexes were optimized *via* DFT computation at the level of the B3LYP functional with D3 dispersion and the 6-31G(d, p) basis set. The buried volume (% V_{bur}) was used to measure the steric environment of the side-arm donors around the Ti active site. The order of % V_{bur} was **6a** (43.1%) $>$ **6b** (41.8%) $>$ **6e** (41.5%), which is opposite to the isotacticities of the corresponding polymers. The -SMe group in **6a** caused obvious steric congestion at the north poles. Considering that atactic poly(1-butene) is generated using **6a**, while an isotactic polymer is preferentially produced by **6e**, it can be preliminarily inferred that the steric hindrance of side-arm donors may be a negative factor affecting isoselectivity. The order of % V_{bur} for possible active species was **Et-6a** (58.8%) $>$ **Et-6b** (56.9%) $>$ **Et-6e** (56.7%), which is consistent with the order of the catalyst precursors.

Conclusions

In summary, an elegant system to generate isospecific C_1 -symmetric active species from tridentate $[\text{O}^-\text{NX}]$ titanium complexes has been discovered, leading to the efficient synthesis of a range of poly(1-butene) samples, from atactic to isotactic (up to 91% *mmmm*), with good polymerization activity (up to $3.41 \times 10^6 \text{ g mol}^{-1} \text{ h}^{-1}$). To the best of our knowledge, no non-metallocene titanium complex catalysts have demonstrated such high activity and isoselectivity in catalyzing the polymer-

ization of α -olefins. Interestingly, isoselectivity can be effectively regulated by modifying one functional group or even one heteroatom of the ligands in this system. In addition, the material properties of poly(1-butene) samples with different isotacticities have been preliminarily investigated, indicating the much better toughness of isotactic poly(1-butene) compared to commercial LDPE. These newly synthesized tridentate $[\text{O}^-\text{NX}]$ titanium complexes bearing different side-arm heteroatoms showed slightly C_1 -symmetric structures in steric maps and single-crystal diffraction analysis. However, this is not sufficient to explain their differential isotactic selectivities. ^{13}C NMR microstructural analysis of poly(1-butene) suggested that the isospecificity results from a mechanism of steric control based on enantiomeric sites. Due to the fact that these trichloride precursors will grow two polymer chains after activation,⁸⁸ explaining their polymerization behavior on the basis of generally accepted symmetry rules⁴² is complicated at present. Experimental and theoretical investigations are currently in progress in order to address the origin of the isoselectivity of these tridentate $[\text{O}^-\text{NX}]$ titanium complexes in our lab.

Author contributions

Conceptualization: Wenjie Tao, Qinggang Wang; experimentation: Guangyu Zhu, Liang Wang, Bo Wang; supervision: Wenjie Tao, Hongbin Hou, Guangqiang Xu, Qinggang Wang; writing: Guangyu Zhu, Wenjie Tao.

Conflicts of interest

There are no conflicts to declare.

Data availability

The data supporting this article have been included as part of the SI.

Supplementary information is available and includes full synthetic sequences, experimental procedures, characterization data and NMR spectra. See DOI: <https://doi.org/10.1039/d5py00583c>.

CCDC 2412497, 2412499, 2412500 and 2412502 contains the supplementary crystallographic data for this paper.^{85a-d}

Acknowledgements

We are grateful for financial support from the National Natural Science Foundation of China (22471282, W. T.), Major Science and Technology Innovation Program of Shandong Province (2022CXGC020604, Q. W.), Taishan Scholars Program of Shandong Province (tstp20240520, Q. W.), Natural Science Foundation of Shandong Province (ZR2023ME008 for G. X., and ZR2023QB156 for G. Z.), and the Scientific Research and Innovation Fund Project of Shandong Energy Research

Institute (SEI I202004, G. X.). We also thank Dr Yanshan Gao for helpful discussion and suggestions.

References

- Y. Men, J. Rieger and J. Homeyer, *Macromolecules*, 2004, **37**, 9481–9488.
- U. W. Gedde, J. Viebke, H. Leijstrom and M. Ifwarson, *Polym. Eng. Sci.*, 1994, **34**, 1773–1787.
- L. Luciani, J. Seppälä and B. Löfgren, *Prog. Polym. Sci.*, 1988, **13**, 37–62.
- Q. Huang, Q. Wu, F. Zhu and S. Lin, *J. Polym. Sci., Part A: Polym. Chem.*, 2001, **39**, 4068–4073.
- S. Abedi and N. Sharifi-Sanjani, *J. Appl. Polym. Sci.*, 2000, **78**, 2533–2539.
- G. Natta, P. Pino, P. Corradini, F. Danusso, E. Mantica, G. Mazzanti and G. Moraglio, *J. Am. Chem. Soc.*, 1955, **77**, 1708–1710.
- G. Natta, *J. Polym. Sci.*, 1955, **16**, 143–154.
- Z. Chen, Y. Mao, Y. Cao, S. Liang, S. Song, C. Ni, Z. Liu, X. Ye, A. Shen and H. Zhu, *Chin. J. Org. Chem.*, 2018, **38**, 2937–2992.
- M. Bochmann, *Organometallics*, 2010, **29**, 4711–4740.
- B. Wang, *Coord. Chem. Rev.*, 2006, **250**, 242–258.
- C. Cobzaru, S. Hild, A. Boger, C. Troll and B. Rieger, *Coord. Chem. Rev.*, 2006, **250**, 189–211.
- F. Focante, P. Mercandelli, A. Sironi and L. Resconi, *Coord. Chem. Rev.*, 2006, **250**, 170–188.
- A. Razavi and U. Thewalt, *Coord. Chem. Rev.*, 2006, **250**, 155–169.
- S. Prashar, A. Antiñolo and A. Otero, *Coord. Chem. Rev.*, 2006, **250**, 133–154.
- J.-Y. Dong and Y. Hu, *Coord. Chem. Rev.*, 2006, **250**, 47–65.
- P. C. Möhring and N. J. Coville, *Coord. Chem. Rev.*, 2006, **250**, 18–35.
- H. Braunschweig and F. M. Breitling, *Coord. Chem. Rev.*, 2006, **250**, 2691–2720.
- S. Lin and R. M. Waymouth, *Acc. Chem. Res.*, 2002, **35**, 765–773.
- E. Y.-X. Chen and T. J. Marks, *Chem. Rev.*, 2000, **100**, 1391–1434.
- G. Fink, B. Steinmetz, J. Zechlin, C. Przybyla and B. Tesche, *Chem. Rev.*, 2000, **100**, 1377–1390.
- G. G. Hlatky, *Chem. Rev.*, 2000, **100**, 1347–1376.
- L. Resconi, L. Cavallo, A. Fait and F. Piemontesi, *Chem. Rev.*, 2000, **100**, 1253–1346.
- G. W. Coates, *Chem. Rev.*, 2000, **100**, 1223–1252.
- H. G. Alt and A. Köpll, *Chem. Rev.*, 2000, **100**, 1205–1222.
- A. L. McKnight and R. M. Waymouth, *Chem. Rev.*, 1998, **98**, 2587–2598.
- W. Kaminsky, *Macromol. Chem. Phys.*, 1996, **197**, 3907–3945.
- G. M. Diamond, R. F. Jordan and J. Petersen, *J. Am. Chem. Soc.*, 1996, **118**, 8024–8033.



28 W. Kaminsky, K. Kölper, H. H. Brintzinger and F. R. W. P. Wild, *Angew. Chem., Int. Ed. Engl.*, 1985, **24**, 507–508.

29 L. Resconi, I. Camurati and F. Malizia, *Macromol. Chem. Phys.*, 2006, **207**, 2257–2279.

30 C. De Rosa, F. Auriemma and L. Resconi, *Angew. Chem., Int. Ed.*, 2009, **48**, 9871–9874.

31 Z. Wen, C. Wu, J. Chen, S. Qu, X. Li and W. Wang, *Polymers*, 2024, **16**, 406–424.

32 C. Chen, *Nat. Rev. Chem.*, 2018, **2**, 6–14.

33 J. P. McInnis, M. Delferro and T. J. Marks, *Acc. Chem. Res.*, 2014, **47**, 2545–2557.

34 M. C. Baier, M. A. Zuideveld and S. Mecking, *Angew. Chem., Int. Ed.*, 2014, **53**, 9722–9744.

35 C. Redshaw and Y. Tang, *Chem. Soc. Rev.*, 2012, **41**, 4484–4510.

36 H. Makio, H. Terao, A. Iwashita and T. Fujita, *Chem. Rev.*, 2011, **111**, 2363–2449.

37 M. Mitani, J. Saito, S. Ishii, Y. Nakayama, H. Makio, N. Matsukawa, S. Matsui, J. Mohri, R. Furuyama, H. Terao, H. Bando, H. Tanaka and T. Fujita, *Chem. Rec.*, 2004, **4**, 137–158.

38 V. C. Gibson and S. K. Spitzmesser, *Chem. Rev.*, 2003, **103**, 283–315.

39 H. Kawamura-Kuribayashi and T. Miyatake, *J. Organomet. Chem.*, 2003, **674**, 73–85.

40 M. Lamberti, M. Consolmagno, M. Mazzeo and C. Pellecchia, *Macromol. Rapid. Commun.*, 2005, **26**, 1866–1871.

41 M. Lamberti, M. Bortoluzzi, G. Paolucci and C. Pellecchia, *J. Mol. Catal. A: Chem.*, 2011, **351**, 112–119.

42 J. A. Ewen, *J. Mol. Catal. A: Chem.*, 1998, **128**, 103–109.

43 G. W. Coates and R. M. Waymouth, *Science*, 1995, **267**, 217–219.

44 W. Kaminsky, O. Rabe, A.-M. Schauwienold, G. U. Schupfner, J. Hanss and J. Kopf, *J. Organomet. Chem.*, 1995, **497**, 181–193.

45 J. A. Ewen, *Macromol. Symp.*, 1995, **89**, 181–196.

46 K. Press, A. Cohen, I. Goldberg, V. Venditto, M. Mazzeo and M. Kol, *Angew. Chem., Int. Ed.*, 2011, **50**, 3529–3532.

47 A. Cohen, J. Kopilov, I. Goldberg and M. Kol, *Organometallics*, 2009, **28**, 1391–1405.

48 Y. Gong, L. Jiang, J. Zhang, S. Liu, P. Braunstein and Z. Li, *ACS Catal.*, 2025, **15**, 8442–8453.

49 S. Kaneko, K. Yasoshima, K. Matsumoto, N. Misawa, Y. Suzuki, N. Koga and M. Nagaoka, *J. Phys. Chem. B*, 2024, **128**, 6178–6188.

50 Y. Kang, H. Wang, X. Li, F. Meng, H. Liu, Y. Xiao, Z. Jiang, H. Gao, C. Liu, F. Wang, Li Pan and Y. Li, *Macromolecules*, 2024, **57**, 4208–4219.

51 Y. Xing, S. Liu and Z. Li, *Polym. Chem.*, 2024, **15**, 4141–4150.

52 J. M. Eagan, J. Xu, R. Di Girolamo, C. M. Thurber, C. W. Macosko, A. M. LaPointe, F. S. Bates and G. W. Coates, *Science*, 2017, **355**, 814–816.

53 K. A. Frazier, R. D. Froese, Y. He, J. Klosin, C. N. Theriault, P. C. Vosejpk, Z. Zhou and K. A. Abboud, *Organometallics*, 2011, **30**, 3318–3329.

54 P. S. Chum and K. W. Swogger, *Prog. Polym. Sci.*, 2008, **33**, 797–819.

55 D. J. Arriola, E. M. Carnahan, P. D. Hustad, R. L. Kuhlman and T. T. Wenzel, *Science*, 2006, **312**, 714–719.

56 T. R. Boussie, G. M. Diamond, C. Goh, K. A. Hall, A. M. LaPointe, M. K. Leclerc, V. Murphy, J. A. W. Shoemaker, H. Turner, R. K. Rosen, J. C. Stevens, F. Alfano, V. Busico, R. Cipullo and G. Talarico, *Angew. Chem., Int. Ed.*, 2006, **45**, 3278–3283.

57 T. R. Boussie, G. M. Diamond, C. Goh, K. A. Hall, A. M. LaPointe, M. Leclerc, C. Lund, V. Murphy, J. A. W. Shoemaker, U. Tracht, H. Turner, J. Zhang, T. Uno, R. K. Rosen and J. C. Stevens, *J. Am. Chem. Soc.*, 2003, **125**, 4306–4317.

58 G. J. Domski, E. B. Lobkovsky and G. W. Coates, *Macromolecules*, 2007, **40**, 3510–3513.

59 L. Annunziata, D. Pappalardo, C. Tedesco and C. Pellecchia, *Macromolecules*, 2009, **42**, 5572–5578.

60 G. Li, C. Zuccaccia, C. Tedesco, I. D'Auria, A. Macchioni and C. Pellecchia, *Chem. – Eur. J.*, 2014, **20**, 232–244.

61 C. De Rosa, R. Di Girolamo, A. B. Muñoz-García, M. Pavone and G. Talarico, *Macromolecules*, 2020, **53**, 2959–2964.

62 G. P. Goryunov, M. I. Sharikov, A. N. Iashin, J. A. M. Canich, S. J. Mattler, J. R. Hagadorn, D. V. Uborsky and A. Z. Voskoboynikov, *ACS Catal.*, 2021, **11**, 8079–8086.

63 J. Tian, Z. Gao, Y. Liu, P. Braunstein, S. Liu and Z. Li, *Inorg. Chem. Front.*, 2024, **11**, 613–623.

64 Y. Chen, S. Zhou, W. Yang and S. Liu, *Organometallics*, 2022, **41**, 3724–3731.

65 A. C. Pinheiro, S. M. da Silva, T. Roisnel, E. Kirilov, J. F. Carpentier and O. L. Casagrande, *New J. Chem.*, 2018, **42**, 1477–1483.

66 L. A. Wright, E. G. Hope, G. A. Solan, W. B. Cross and K. Singh, *Organometallics*, 2016, **35**, 1183–1191.

67 R. Zhao, T. Liu, L. Wang and H. Ma, *Dalton Trans.*, 2014, **43**, 12663–12677.

68 Y. Wang, W. Zhang, W. Huang, L. Wang, C. Redshaw and W.-H. Sun, *Polymer*, 2011, **52**, 3732–3737.

69 W. Huang, W. Zhang, S. Liu, T. Liang and W.-H. Sun, *J. Polym. Sci., Part A: Polym. Chem.*, 2011, **49**, 1887–1894.

70 M. Xue, L. Lei, S. Ren, T. Li, Q. You and G. Xie, *Polymer*, 2023, **277**, 125995.

71 L. Ji, J.-S. Liu, X.-Y. Wang, J.-F. Li, Z. Chen, S. Liao, X.-L. Sun and Y. Tang, *Polym. Chem.*, 2019, **10**, 3604–3609.

72 C. Xu, Z. Chen, Q. Shen, X.-L. Sun and Y. Tang, *J. Organomet. Chem.*, 2014, **761**, 142–146.

73 Z. Wang, A.-Q. Peng, X.-L. Sun and Y. Tang, *Sci. China: Chem.*, 2014, **57**, 1144–1149.

74 D.-W. Wan, Z. Chen, Y.-S. Gao, Q. Shen, X.-L. Sun and Y. Tang, *J. Polym. Sci., Part A: Polym. Chem.*, 2013, **51**, 2495–2503.

75 Z. Chen, J.-F. Li, W.-J. Tao, X.-L. Sun, X.-H. Yang and Y. Tang, *Macromolecules*, 2013, **46**, 2870–2875.

76 P. Tao, X.-Y. Tang, B.-X. Li, J.-Y. Liu and Y.-S. Li, *Dalton Trans.*, 2012, **41**, 7390–7398.



77 X. Wang, M.-M. Sit, J. Sun, Y. Tang and Z. Xie, *Acta Chim. Sin.*, 2012, **70**, 1909–1916.

78 X.-H. Yang, Z. Wang, X.-L. Sun and Y. Tang, *Dalton Trans.*, 2009, 8945–8954.

79 X.-H. Yang, C.-R. Liu, C. Wang, X.-L. Sun, Y.-H. Guo, X.-K. Wang, Z. Wang, Z. Xie and Y. Tang, *Angew. Chem., Int. Ed.*, 2009, **48**, 8099–8102.

80 X.-H. Yang, X.-L. Sun, F.-B. Han, B. Liu, Y. Tang, Z. Wang, M.-L. Gao, Z.-W. Xie and S.-Z. Bu, *Organometallics*, 2008, **27**, 4618–4624.

81 C. Wang, Z. Ma, X.-L. Sun, Y. Gao, Y.-H. Guo, Y. Tang and L.-P. Shi, *Organometallics*, 2006, **25**, 3259–3266.

82 W.-Q. Hu, X.-L. Sun, C. Wang, Y. Gao, Y. Tang, L.-P. Shi, W. Xia, J. Sun, H.-L. Dai, X.-Q. Li, X.-L. Yao and X.-R. Wang, *Organometallics*, 2004, **23**, 1684–1688.

83 A. Ciccolella, E. Romano, V. Barone, C. De Rosa and G. Talarico, *Organometallics*, 2022, **41**, 3872–3883.

84 C. De Rosa, R. Di Girolamo and G. Talarico, *ACS Catal.*, 2016, **6**, 3767–3770.

85 (a) ; CCDC 2412497 (for **6a**): Experimental Crystal Structure Determination, DOI: [10.5517/ccdc.csd.cc2lzdhh](https://doi.org/10.5517/ccdc.csd.cc2lzdhh); (b) CCDC 2412499 (for **6c**): Experimental Crystal Structure Determination, DOI: [10.5517/ccdc.csd.cc2lzdkk](https://doi.org/10.5517/ccdc.csd.cc2lzdkk); (c) CCDC 2412500 (for **6d**): Experimental Crystal Structure Determination, DOI: [10.5517/ccdc.csd.cc2lzdll](https://doi.org/10.5517/ccdc.csd.cc2lzdll); (d) CCDC 2412502 (for **6e**): Experimental Crystal Structure Determination, DOI: [10.5517/ccdc.csd.cc2lzdnn](https://doi.org/10.5517/ccdc.csd.cc2lzdnn).

86 A. C. K. Tashiro, J. Hu, H. Wang, M. Hanesaka and A. Saiani, *Macromolecules*, 2016, **49**, 1392–1404.

87 L. Falivene, Z. Cao, A. Petta, L. Serra, A. Poater, R. Oliva, V. Scarano and L. Cavallo, *Nat. Chem.*, 2019, **11**, 872–879.

88 Y. Suzuki, S. Kinoshita, A. Shibahara, S. Ishii, K. Kawamura, Y. Inoue and T. Fujita, *Organometallics*, 2010, **29**, 2394–2396.

